

ORIGINAL ARTICLE OPEN ACCESS

# Preclinical Evaluation of Closed Incisional Negative Pressure Therapy on Post-Surgical Oedema and Lymphatic Activity

John C. Rasmussen<sup>1</sup>  | Marisa Schmidt<sup>2</sup>  | Janelle E. Morton<sup>1</sup> | Samantha Mann<sup>2</sup>  | Kristine Kieswetter<sup>2</sup> | Eva M. Sevick-Muraca<sup>1</sup>

<sup>1</sup>Center for Molecular Imaging, The Brown Foundation Institute of Molecular Medicine, University of Texas Health Science Center at Houston, Houston, Texas, USA | <sup>2</sup>Medical Surgical Business, Solventum, San Antonio, Texas, USA

**Correspondence:** John C. Rasmussen ([john.rasmussen@uth.tmc.edu](mailto:john.rasmussen@uth.tmc.edu)) | Marisa Schmidt ([mschmidt12@solventum.com](mailto:mschmidt12@solventum.com))

**Received:** 20 September 2024 | **Revised:** 10 December 2024 | **Accepted:** 17 December 2024

**Funding:** This work was supported by Solventum.

**Keywords:** incisional negative pressure therapy | indocyanine green | lymphatic | near-infrared fluorescence imaging | surgical recovery

## ABSTRACT

Closed incisional Negative Pressure Therapy (ciNPT) has demonstrated improved post-surgical healing with reduced oedema and hematoma/seroma formation in patients. The underlying mechanism of action is poorly understood, although evidence indicates that lymphatics play a role. The effects of ciNPT on oedema and lymphatic recovery were assessed following bilateral, surgical undermining of swine mammary tissues. One incision was treated with ciNPT, and the control covered with clear dressing. Near-infrared fluorescence imaging was used to visualise lymphatic activity. Oedema and lymph node size were measured using ultrasound. LYVE-1 and podoplanin were quantified with ELISA. Analysis of lymphatic activity revealed a contralateral effect of ciNPT on control sites. Statistically higher pulsatile rates were observed at both incisions when ciNPT was active, compared with when it was removed. Separate evaluations with dressings off and on showed no differences between treatments. While not significant, lower surgical site oedema, lymph node volume, and incidence/severity of seroma were observed in treated sites along with increased lymphatic vessel markers in lymph draining tissues. Taken together, evidence suggests that ciNPT may influence watersheds outside the treated area. Similar systemic impacts owing to manual lymphatic drainage have previously been reported in healthy individuals and those with cancer-related lymphedema.

## 1 | Introduction

Oedema is a common post-surgical complication arising from the body's natural inflammatory responses due to incisions, tissue manipulation, and closure methods. In most cases, inflammation is moderate and resolves within a few weeks with minimal intervention such as ice and compression. However, prolonged or excessive tissue swelling may increase pressure along the incision line, leading to dehiscence and increased risk of infection. Additionally, the accompanying pain and discomfort from

excessive post-surgical oedema can inhibit muscle recruitment, limiting mobility, and subsequently slowing the healing process.

In the 1930s researchers determined that the lymphatics played a primary role in the removal of fluid from oedematous tissue [1]. Today, a number of strategies, including the traditional recommendation of rest, ice, compression, elevation (RICE) [2], are recommended to help prevent fluid accumulation and manage post-operative oedema, but these methods do not focus on stimulating lymphatic activity. Approaches involving physical

John C. Rasmussen and Marisa Schmidt contributed equally to this work.

This is an open access article under the terms of the [Creative Commons Attribution-NonCommercial-NoDerivs](https://creativecommons.org/licenses/by-nc-nd/4.0/) License, which permits use and distribution in any medium, provided the original work is properly cited, the use is non-commercial and no modifications or adaptations are made.

© 2025 The Author(s). *International Wound Journal* published by Medicalhelplines.com Inc and John Wiley & Sons Ltd.

## Summary

- Closed incisional Negative Pressure Therapy (ciNPT) engages the lymphatics to promote oedema resolution and post-surgical recovery.
- The effects of ciNPT on oedema and lymphatic recovery were assessed following lymphatic vessel transection and bilateral mammary tissue undermining in eight female swine. Surgical sites were treated with either ciNPT or covered with a clear film dressing after surgical closure. Near-infrared fluorescence imaging and indocyanine green were used to visualise lymphatic activity. Areas of fluid accumulation surrounding the surgical site and tissue thickness measurements were performed to assess oedema, and lymphatic vessel markers were quantified with ELISA.
- The study was concluded early after interim analysis revealed that the ciNPT device appeared to stimulate lymphatic function systemically. Analysis of lymphatic activity revealed no significant differences between treatments at each study visit; however, statistically higher pulsatile rates were observed for both treatments when ciNPT was active, compared with when it was removed. Despite seeing slight improvements for ciNPT in oedema measures, seroma scoring, and lymphatic vessel markers, no significant differences were found between treatments, possibly owing to small sample size ( $n = 8$ ). Taken together, evidence suggests that, in swine models, ciNPT may have a systemic affect, influencing watersheds outside the treated area.

manipulation of tissues, including ultrasound, manual lymphatic drainage, and topical negative pressure therapy, have been shown to encourage lymphatic activity and improve oedema resolution [3].

Since their introduction and clinical adoption, closed incision Negative Pressure Therapy (ciNPT) systems have reduced the incidence of incision-related complications, particularly of surgical site infection and wound dehiscence in many closed-incision surgical applications including breast surgery [4, 5], orthopaedic trauma [6, 7], and laparotomies [8]. Other reported improvements include reduced incidence of hematoma/seroma [4, 9–11] and wound necrosis [4, 5], reduced oedema [11, 12], and improved range of motion [11]. While there is clearly a lower incidence of healing complications, the underlying physiologic mechanism(s) of action behind these improvements is poorly understood. Increased blood flow, as measured using Doppler imaging, as well as increased levels of angiogenesis-related growth factors, including vascular endothelial growth factor (VEGF), epidermal growth factor (EGF), platelet-derived growth factor (PDGF), and angiotensin-2, have been reported after commencing negative pressure wound therapy ( $-125$  mmHg pressure) in a study of subjects with infected wounds [13–15], though reduced blood flow has been reported at higher suction pressures in another study of healthy subjects using radioisotope perfusion to assess perfusion under the dressing [16]. Other proposed physiologic mechanisms include the reduction of swelling,

wound exudate removal, and, owing to the associated dressings, decreased exposure to bacterial contamination [17], all of which promote wound healing.

As with open wounds, the application of negative pressure may optimise the healing environment of closed incisions by increasing fluid transport via the lymphatics, as measured by increased lymph pumping rates, to aid in the reduction of post-surgical oedema. This work assesses the impact of ciNPT on oedema resolution and lymphatic pumping function and recovery, following bilateral, surgical transection of lymphatic vessels and mammary tissue undermining in a healthy swine model, using near-infrared fluorescence lymphatic imaging (NIRF-LI). NIRF-LI has previously been used to assess lymphatic (dys)function in murine [18] and porcine [19, 20] models, as well as in human [21, 22] health and disease.

## 2 | Materials and Methods

### 2.1 | Materials

A  $15.5 \times 10$  cm polyurethane film with acrylic adhesive (3M Tegaderm Transparent Film Dressing, Solventum, St. Paul, MN) was placed over the control incision site before applying the test article on the contralateral incision.

A 13 cm, ciNPT dressing/device (3M Prevena Peel and Place Incision Dressing, Solventum, St. Paul, MN) served as the experimental test article. The foam dressing was placed over the contralateral incision to allow negative pressure to be applied. Due to the limited distance between the two sites, 1–2 cm of the test article adhesive film border overlapped the previously covered control site.

The test article consists of an interfacial fabric layer comprised of 0.019% ionic silver bonded to a reticulated open cell foam dressing encased in a polyurethane film with acrylic adhesive. A small negative pressure pump (3M Prevena 125 Therapy unit, Solventum, St. Paul, MN) was attached to the dressing and set to maintain a constant  $-125$  mmHg pressure over the course of the study.

### 2.2 | Intradermal Injections

Indocyanine green (ICG; Diagnostic Green, Farmington Hills, MI) was reconstituted per the manufacturer's instructions (25 mg ICG into 10 mL sterile water) and then serially diluted to obtain a final concentration of  $250 \mu\text{g}/\text{mL}$  (1 mL stock ICG solution into 9 mL sterile saline).

For each NIRF-LI imaging session, intradermal injections of  $50 \mu\text{L}$  of the diluted ICG solution provided lymphatic contrast to assess function. In Fig 1,  $100 \mu\text{L}$  injections of diluted ICG (used at baseline Day  $-4$  and Day 0) provided excessive contrast that made visualisation of lymphatic 'pumping' difficult and hence, subsequent studies employed the smaller volume. Because lymphatic anatomy differed between animals, imaging on Day  $-4$  initially employed a  $< 10 \mu\text{L}$  intradermal injection of diluted ICG above the second row of teats. If the

injection site drained cranially or merged with a neighbouring lymphatic vessel, a new injection site was selected. Once an acceptable drainage pattern was identified the remaining dosage, up to 50  $\mu$ L, was administered. Final injection sites were located such that, when possible, lymphatic vessels were visible on the medial and lateral aspects of the bilateral sets of teats. At subsequent imaging sessions, the injections were performed at the same four identified locations based on visualisation of the residual ICG at the depot either with the eye (green colour) or fluorescent signal with NIRF-LI (bright spot in image).

### 2.3 | Animal Studies

All animal procedures were humanely performed under veterinarian care with approval from the University of Texas Health Science Center at Houston's Institutional Animal Care and Use Committee in compliance with the institution's guidelines and those outlined in the 'Guide for the Care and Use of Laboratory Animals' [23]. The study was performed in a swine model owing to their size, which allowed the placement of unaltered ciNPT devices, and the similarities between porcine and human lymphatics [24, 25], including their response to physiotherapy [20, 26]. Using lymphatic activity (i.e., propulsion rate) data from an earlier unpublished 2-animal pilot study, the treatment effect size was assumed to be 0.29. With a fixed level of significance  $\leq 0.05$  and power  $\geq 80\%$ , a power calculation indicated that a sample size of  $n = 10$  would be required to demonstrate significance of the primary measure of lymphatic activity. Insufficient data was available during the study design to conduct power calculations of the secondary measures including oedema and biomarker levels. However, after eight animals, the study was concluded early as it became clear that statistical significance would not be achieved for lymphatic activity and imaging two additional animals would not be prudent. A cohort of eight Yorkshire-cross swine (37.3–60.9 kg) with non-pigmented bellies were anaesthetised (Telazol 6–8 mg/kg and atropine 0.04 mg/kg), intubated, and maintained supine with isoflurane and saline drip for fluid homeostasis. Electrocardiography, heart rate, oxygen saturation, and body temperature were monitored during imaging and the surgical procedure. After procedures were completed at each imaging session, animals were allowed to recover. After the procedures on Day 9, animals were euthanized using 0.22 mg/kg pentobarbital sodium and tissue samples were collected.

Lymphatic imaging was conducted during five separate imaging sessions over 13 days. At the first imaging session (Day -4), baseline NIRF-LI was performed to locate caudally draining injection sites and assess baseline lymphatic drainage. Ultrasound was used to assess the skin thickness near the proposed surgical sites and the volume of the draining lymph nodes. After 4 days (Day 0), baseline NIRF-LI was repeated followed by bilateral surgery to undermine mammary tissues and sever the draining lymphatic vessels of the teats nearest the umbilicus. A semi-circumferential incision was made caudal to the teat using a modified method described by Ashitate et al. [27] Undermining was performed using blunt dissection, and any large blood vessels were left intact. NIRF-LI was used to identify lymph vessels comingled with spared veins for transection. After confirmation of lymphatic transection, incisions were closed with absorbable suture material. One surgical site was randomly chosen for treatment using ciNPT, while the contralateral site was covered with the control dressing. The animal was fitted with a custom neoprene jacket with a wide belly band to protect the surgical sites, and hook and loop fasteners were used to secure the ciNPT device onto the jacket to allow for continuous application of negative pressure when the animal was returned to housing.

To longitudinally assess lymphatic drainage, NIRF-LI was conducted 2, 6, and 9 days (Day 2, Day 6, and Day 9) after surgery. On these days, animals were anaesthetised and intubated. Then NIRF-LI was performed with and without ciNPT and control dressings in place; ultrasound imaging was utilised to assess the skin thickness at the surgical sites and the draining lymph node volumes. After experimental procedures were complete, the swine were allowed to recover and returned to housing. On Day 9 animals were humanely euthanized, and tissues were collected for histology and proteomic assessment. Figure 1 provides an overview of the experimental design and procedures performed at each of the five imaging sessions over the course of the study. Individual procedures are described below in more detail.

### 2.4 | NIRF-LI Imaging and Analysis

NIRF-LI was accomplished using a custom-built fluorescence imaging system described elsewhere [28]. Briefly, the belly of each animal was illuminated with the diffuse output of a 780 nm laser diode with a maximum fluence  $< 1.9$  mW/cm<sup>2</sup> measured 30 cm from the aperture. The resultant fluorescent

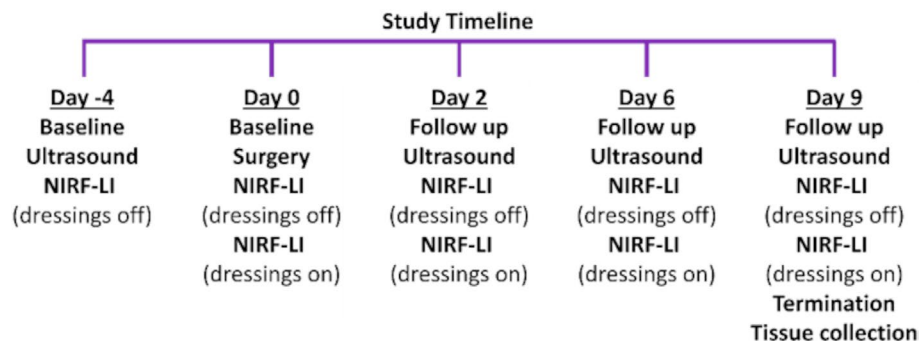


**FIGURE 1** | Schematic illustrating the study timeline and major events occurring at each study visit.

signal was filtered using a set of 830 nm bandpass filters and collected using an intensified, scientific complementary metal-oxide semiconductor (sCMOS) camera. With image exposure times of 200 ms and frame rates of 2–3 frames per sec, images and movies of lymphatic propulsion from the injection sites to the draining lymph node basins were obtained. Images were acquired for approximately 20 min with and without the dressings in place. Injection sites, and occasionally the surgical sites, were temporarily covered during imaging to prevent image oversaturation and to facilitate the visualisation of the dimmer lymphatic vessels.

For data analysis purposes, the imaging area on the abdomen was divided into four quadrants, left and right of the midline and above (upstream) and below (downstream) the surgical sites. Depending on the placement of the ciNPT device, left and right sides were identified as 'ciNPT' or 'Control.' NIRF-LI images were assessed by drawing three consecutive regions of interest (ROIs) along each section of lymphatic vessel and plotting the average intensity of each ROI as a function of time. Peaks in the average fluorescent intensity, representing pumping movement of ICG-laden packets of lymph fluid across the ROI (lymphatic propulsion), were identified as being forward or backward moving or static depending on the direction the peak appeared to move between consecutive ROIs (Figure 4B–D). The overall number of propulsion events, regardless of direction or vessel, observed in each quadrant were totalled. Propulsion rates were calculated by dividing the total number of observed propulsion events in each quadrant by the elapsed time (approximately 20 min) for the corresponding image sequence. The numbers of events and imaging times from Day –4 and the pre-surgical imaging on Day 0 were averaged to obtain an average baseline measurement. Statistical comparisons were made between treatments at each study visit on data collected with or without dressings in place. Analysis of lymphatic recovery over time was performed for upstream and downstream locations using combined treatment data. To determine whether differences exist between datasets collected with and without dressings in place, lymphatic activity rates were compared using the downstream quadrants on Days 2, 6, and 9 as propulsion was typically absent on Day 0 post-surgery.

The extent or area of lymphatic pooling around each surgical site was calculated using ImageJ (National Institutes of Health, USA). This was done by auto-adjusting the brightness and contrast of the image and then drawing an ROI around each pooled fluorescent area around the surgical sites. The area (i.e., the number of pixels within each ROI) was then calculated using the Measure function. The NIRF-LI images used to assess lymphatic pooling were selected from a set of images acquired approximately 25 min after injection and before the dressings were replaced. A representative analysed image can be found in Figure 6A.

## 2.5 | Ultrasound Imaging

After NIRF-LI imaging on Day –4, ultrasound (L7 scanner; Clarius, Vancouver, BC, CA and Z6Vet; Mindray, Mahwah, NJ, USA) was performed to assess oedema by measuring the baseline thickness of the skin and subcutaneous tissues at the surgical sites. The fluorescent inguinal lymph nodes were also

visualised, and their transverse width, sagittal width, and transverse height measured. To measure the changes during recovery, ultrasound measurements were repeated on Days 2, 6, and 9. As baseline measurements were previously recorded on Day –4, and to minimise sedation time, ultrasound was not repeated on Day 0. The volume of the lymph nodes at each visit was approximated as an ellipsoid as shown in the equation below, where  $a$  is half the measured transverse width,  $b$  is half the measured transverse height, and  $c$  is half the measured sagittal width.

$$\text{LN Volume} = \frac{4}{3}\pi abc$$

Oedema at the surgical site was evaluated using ultrasound tissue thickness measurements (the distance from the surface of the skin down to the first fascial layer). The percent change in lymph node volume and skin thickness were computed with respect to the baseline measurements.

## 2.6 | Histology/Proteomics

Tissues from each surgical site (incision) as well as naïve tissues cranial (upstream) and caudal (downstream) to the surgical sites were collected, fixed in 10% Neutral Buffered Formalin (NBF), and sent for histopathological processing and evaluation (StageBio, Frederick, MD, USA). Incision sites were trimmed to sample one section through the upper and one through the lower regions of the incision. Both naïve sites were trimmed to one section each. All sites were embedded in paraffin, sectioned, and stained with haematoxylin and eosin (H&E) for blinded evaluation by a board-certified veterinary pathologist. The evaluation for seroma severity was based on a 5-point semi-quantitative scale.

Additionally, biopsies were collected from each location and snap frozen in liquid nitrogen. Biopsies were cut and weighed in preparation for protein extraction. Tissue lysate was prepared by adding minced tissue to Lysing Matrix D tubes (MP Biomedicals, Irvine, CA, USA) containing T-PER Extraction Reagent and Halt Protease Inhibitor Cocktail (Pierce Biotechnology, Rockford, IL, USA). The tubes were agitated with a Fast Prep 24 System (MP Biomedicals) homogeniser, and samples were iced between homogenisation cycles.

The tubes were centrifuged to collect supernatant. Isolated protein was stored at –80°C prior to analysis. Total protein concentration was determined via Pierce Bicinchoninic Acid (BCA) assay (Pierce Biotechnology). Each sample was analysed in technical triplicate using Porcine Podoplanin (PDPN) and Lymphatic Vessel Endothelial Hyaluronic Acid Receptor 1 (LYVE1) ELISA Kits (MyBioSource, San Diego, CA, USA). Optical density was read using a SpectraMax i3x plate reader and raw data exported for analysis in JMP (version 17.0.0, SAS Institute Inc., Cary, NC, USA). Normalised proteomic data is presented as a ratio of the amount of detected analyte per gram of total protein relative to BCA. Data were evaluated to look for differences between treatment and control at each treatment location (upstream, incision, and downstream) and between locations.

## 2.7 | Statistical Analysis

All data are reported as means with standard deviation (SD). Analysis was performed using JMP (version 18.0.1, JMP Statistical Discovery LLC, Cary, NC, USA). The Shapiro–Wilk goodness-of-fit test was used to determine normality. Nonparametric (non-normal) distribution measures include lymphatic activity, seroma scores, LYVE-1, podoplanin, lymphatic pooling, and skin thickness. Lymph node volume was normally distributed, and means were compared using ANOVA. Nonparametric comparisons were performed using the Wilcoxon/Kruskal Wallis method with alpha set at 0.05 and Steel-Dwass was used for pairwise comparisons to control the overall error rate.

## 3 | Results

The course of NIRF-LI, ultrasound imaging, surgery, and ciNPT treatment was successfully completed for each animal with no study-related adverse events reported.

Lymphatic vessels, with active lymphatic propulsion, draining from injection sites to the inguinal lymph nodes were observed in each of the swine. Figure 2 illustrates the location of injection sites, baseline lymphatic vessels, inguinal lymph nodes, surgical sites, and the placement of the ciNPT device. Despite each animal having unique vessel patterns, consistent lymphatic watershed activity was observed as lymph was propelled from cranial injection sites to caudal draining lymph nodes. Interestingly, one animal (Fig 2, Figure 2 arrow) had an unusual lymphatic vessel visualised on Day –4 and Day 0 (pre-surgery), that appeared to originate from the left inguinal lymph nodes with lymph moving upstream towards the injection sites.

Surgical incisions were typically located near the first pair of teats at or below the umbilicus. Ensuring that all the lymphatic vessels crossing the surgical sites were severed was challenging and required isolating the subcutaneous abdominal vein crossing the surgical site to minimise the apparent recruitment of collateral lymphatic vessels located in its proximity. After surgery on Day 0 the downstream lymphatic vessels generally

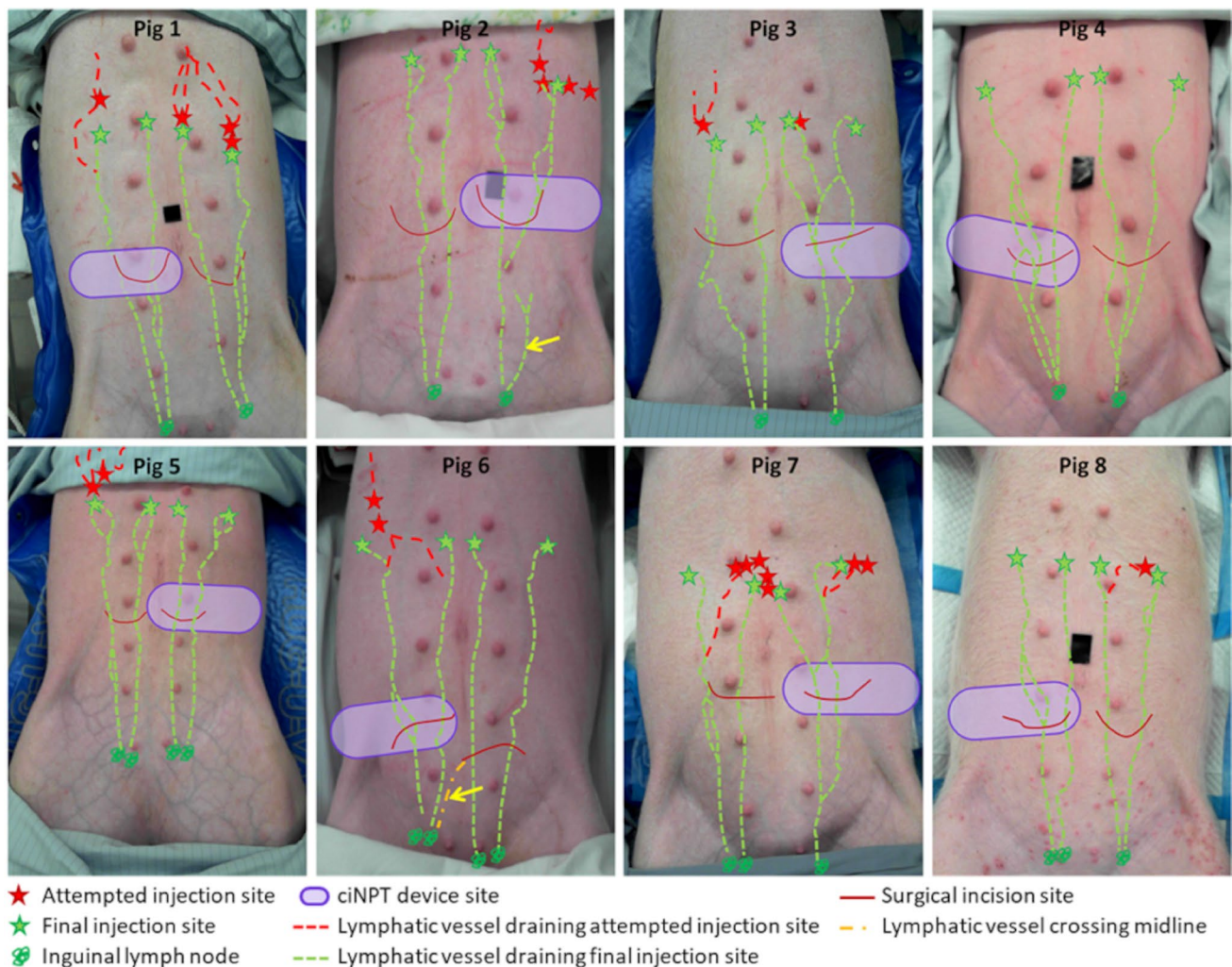


**FIGURE 2** | Day 0 pre-surgical photographs of Pigs 1–8 with illustrations identifying ICG injection sites, draining lymphatic vessels, collecting inguinal lymph nodes, surgical incision sites, and ciNPT placement site. Arrows show (Pig 2) a lymph vessel that appears to originate from the inguinal lymph node with retrograde, cranial flow, and (Pig 6) a lymph vessel crossing the midline from the control to the ciNPT side. Black vinyl tape shown on Pigs 1, 2, 4, and 8 were used to facilitate camera focus.

became dimmer as the ICG-laden lymph cleared and was not replenished by the upstream lymphatics as shown in Figure 3. On Day 2 the downstream lymphatics were still dim relative to the upstream lymphatics and baseline but had observable propulsion events. By Day 6 the downstream lymphatics were visible though the lymphatic vessels on the treated side were visible several minutes sooner than those on the control side. By Day 9, the downstream lymphatic vessels were readily visible regardless of treatment and often additional collateral lymphatic vessels, which were not observed at baseline, were visible. While collateral lymphatic vessels were frequently observed downstream from the surgical sites, during follow up visits, only one animal (Fig 6, Figure 2 arrow) had a collateral lymphatic vessel that crossed the midline of the animal from the control to the treatment side. Because it was unclear whether the propulsion events observed in the crossover vessel should be assigned to the downstream Control or ciNPT quadrant, they were excluded from analysis.

The directionality of the propulsion events was determined based on the movement of the peaks or valleys of fluorescence intensity along the lymphatic vessel as shown in Figure 4. Forward moving propulsion events presented as a peak in the average fluorescence intensity that moved from the first ROI to third ROI in the direction of the inguinal lymph nodes as would be expected in a healthy, undamaged lymphatic vessel. Backward moving propulsion events frequently presented as a valley (dimmer fluorescent signal) in the average fluorescence intensity which moved from ROI to ROI towards the injection sites. While often interspersed between forward events, backward moving events appeared to be independent of forward events and thus were not considered to be lymphatic reflux where a portion of a forward moving event simultaneously drains backward along the lymphatic vessel as reported previously in humans [29]. Peaks that did not move between ROIs, whether forward or backward, were noted as static, and, at least in some cases, may result from lymphatic vessel spasms related to surgical trauma rather than a true propulsion

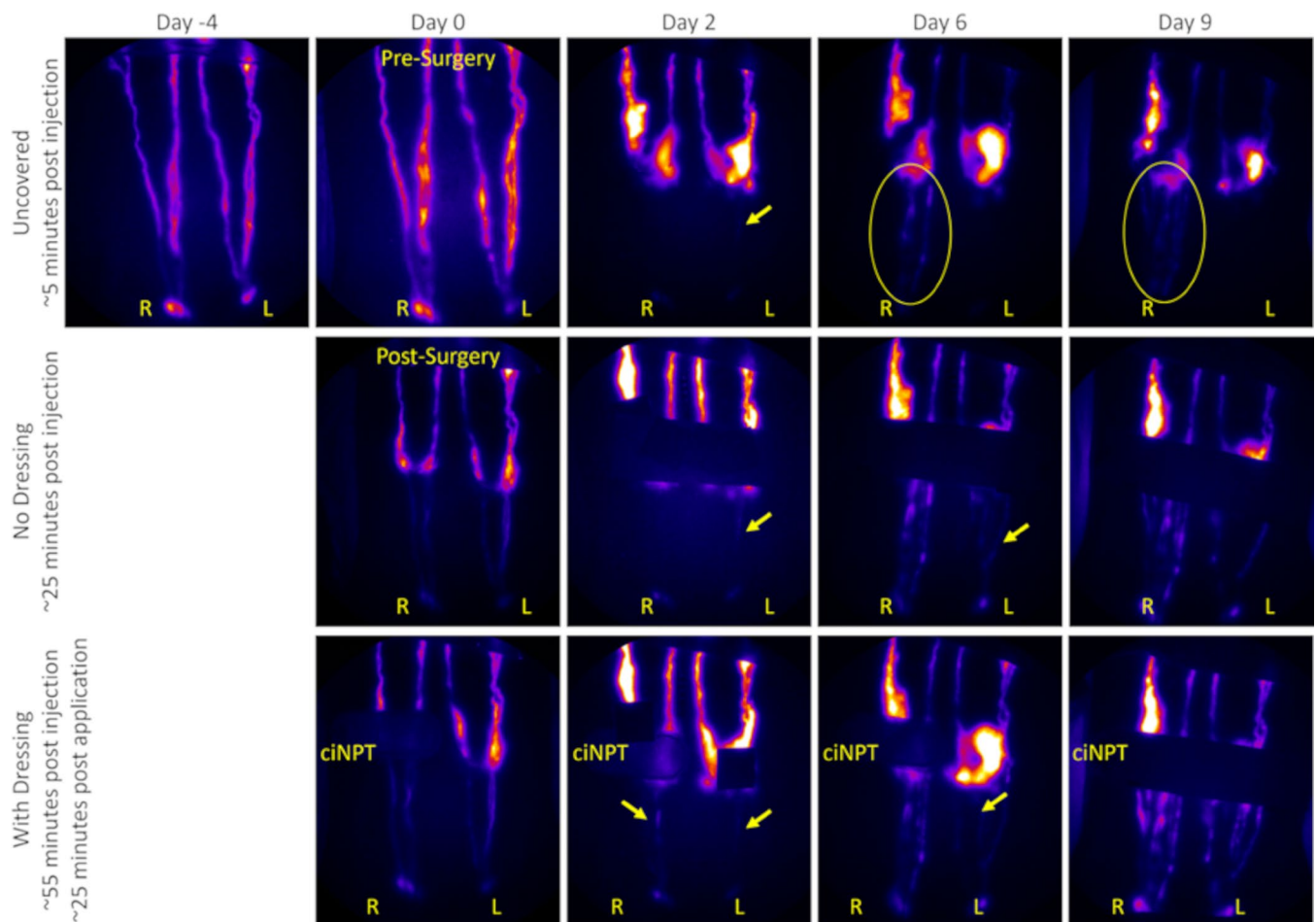


**FIGURE 3** | Example NIRF-LI images (Fig 1) showing typical lymphatic recovery following surgery. The top row presents images from each study visit, taken ~5 min post injection. The second row images, without the device applied, were collected ~25 min post injection. The third row images show the ciNPT device on the animal's right side, collected ~25 min after dressing application. R and L indicate the right and left sides of the animal, respectively. The arrows indicate faint lymphatic vessels that may not be visible in print. While a vessel was faintly observed on the left, control side at Day 2, the fluorescence was likely residual ICG from Day 0 as the vessel intensity did not increase over the imaging period and no propulsion events were observed. The circles highlight lymphatic vessels that are visible on the treated side within minutes of injection. Dark areas covering surgical sites from Days 2, 6, and 9 (with and without dressings) are either paper towels or an alcohol wipe packet placed atop overly bright areas of lymphatic pooling to prevent oversaturation of the camera. NIRF-LI images are displayed in pseudo colour with adjusted brightness and contrast to enhance the visualisation of dimmer lymphatic vessels.

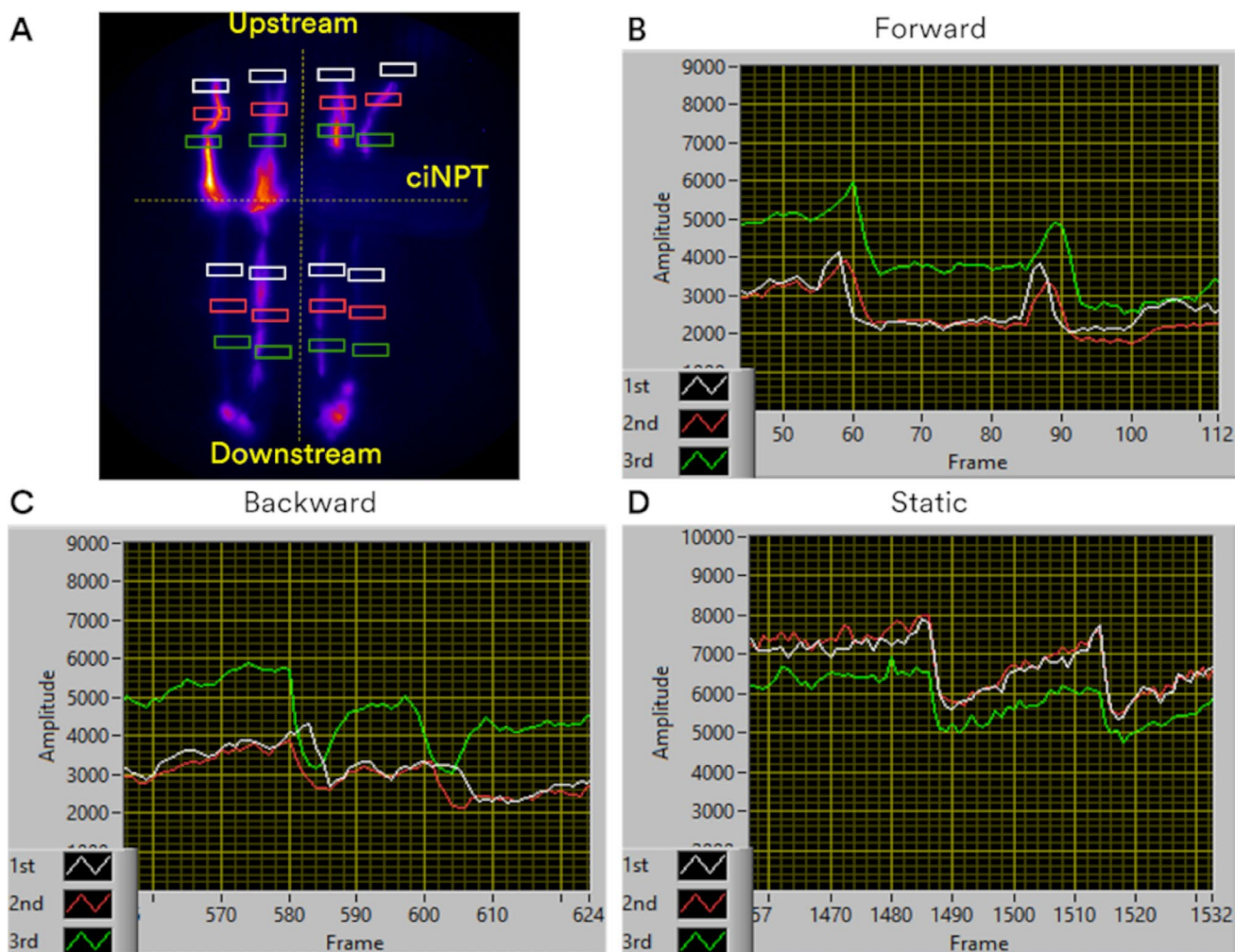


**FIGURE 4** | (A) Image illustrating the quadrants of the pig belly used to aggregate contractile events as well as example locations of ROIs along each vessel (image of Fig 5; Day 0, post-surgery with ciNPT in place). Example plots of the fluorescence intensity fluctuations that attend apparent lymphatic contractile events corresponding to three consecutive ROIs drawn along a vessel segment. (B) Forward movement of fluorescence from the 1st ROI (white) through the 2nd (red) and then 3rd (green) ROIs, (C) backward movement with dimmer fluorescence from the 3rd to the 1st ROI, and (D) static fluorescence occurring in consecutive ROIs simultaneously.

event (Figure 4). All events, forward, backward, or static, were added to assess total lymphatic activity for data analysis.

While care was taken to isolate the vein from the surrounding tissues, including the use of NIRF-LI to verify that no visible fluorescent lymphatic vessels crossed the surgical site, a small number (<6) of propulsion events were observed in downstream quadrants of three animals (Figs 2, 4, and 5) while 67 were observed in Fig 7 after surgical closing on Day 0. In all but one (Fig 4) of these four animals, these downstream propulsion events were identified as static and may result from lymphatic vessel spasms related to surgical trauma rather than representing true propulsion events. In Fig 6 one non-static propulsion event was observed in each of the downstream quadrants post-surgery (Day 0).

### 3.1 | Lymphatic Activity Increased Significantly When Therapy Was Active

After surgery, upstream lymphatic activity rates decreased over time (30%–56%) and never recovered to baseline levels

( $p \leq 0.0157$ ). After lymphatic transection on Day 0, downstream activity dropped to near zero, as expected, and remained significantly lower than baseline on Day 2 ( $p < 0.01$ ). Activity rates recovered to baseline by Day 6 ( $p = 0.6382$ ) and then significantly exceeded baseline by Day 9 ( $p = 0.0096$ ). While it was anticipated that downstream rates on the ciNPT side would exceed those on the control side, as seen on Day 6 ( $p = 0.0406$ ) with dressings in place, it was surprising to note that control exceeded ciNPT on Days 2 and 9 though differences were not significant ( $p > 0.05$ ). Mean upstream and downstream lymphatic propulsion rates are shown in Figure 5A–C.

As downstream rates were higher with dressings in place regardless of treatment assignment, pooled treatment data was used for analysis of dressings in place (on) versus removed (off). Significantly increased lymphatic propulsion occurred when both dressings were in place and the ciNPT –125 mmHg therapy was active (On) as compared with when they were removed (Off);  $p = 0.0224$  (Figure 5D). Because the presence of the clear film control is unlikely to have impacted lymphatic pumping, it

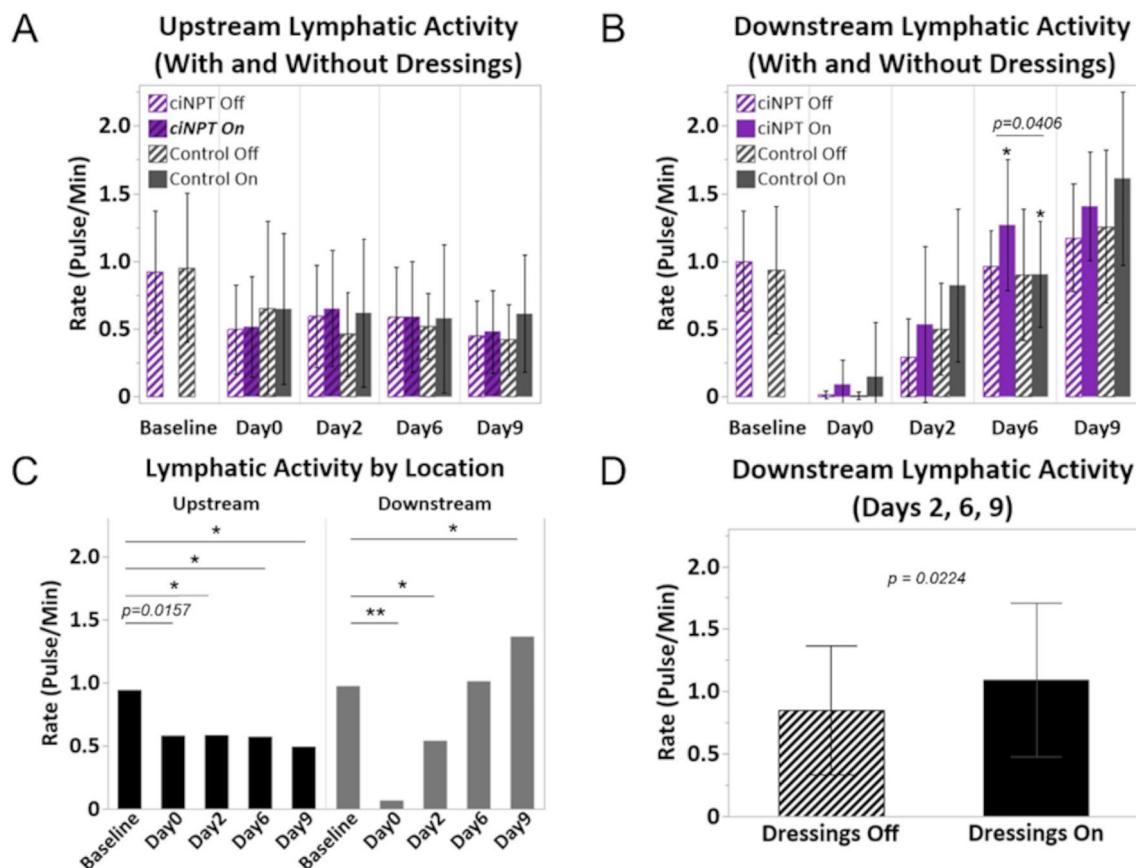


**FIGURE 5** | Plots of the mean upstream (A) and downstream (B) rates as a function of Day, Treatment, and Dressings. The hashed bars indicate when dressings are not in place (Off) and solid bars indicate when dressings are in place and the ciNPT  $-125\text{mmHg}$  therapy is active (On). The only significant difference observed between treatments at each study visit (with or without dressings in place) was observed on Day 6, downstream, with both ciNPT and control dressings in place ( $p=0.0406$ ). (C) Lymphatic activity upstream from the incision decreased significantly from baseline over time and did not recover ( $p\leq 0.0157$ ). Downstream rates dropped significantly after surgery on Days 0 and 2 ( $p<0.01$ ), recovered to baseline levels by Day 6 ( $p=0.6382$ ), and significantly exceeded baseline activity by Day 9 ( $p<0.0001$ ). (D) Analysis of overall downstream lymphatic activity from Days 2, 6, and 9 comparing dressings Off versus On, revealed that lymphatic activity was significantly higher when dressings were On ( $p=0.0224$ ). Data presented are means  $\pm$  standard deviation. \* $p<0.01$ ; \*\* $p<0.0001$ .

is likely that the ciNPT device stimulated lymphatic propulsion over the broader region or perhaps even systemically. Similar increases in propulsion rates have been observed systemically in humans during manual lymphatic drainage treatment of lymphedema [26].

### 3.2 | Lower Observations of Oedema With ciNPT

Lower measures of oedema and inflammation were observed with ciNPT treatment, but differences were not significant, likely due to the relatively small sample size ( $n=8$ ). Areas of lymphatic pooling (in  $\text{cm}^2$ ) on Days 2, 6, and 9 were  $35.9 \pm 14.7$ ,  $36.3 \pm 18.4$ , and  $24.9 \pm 10.4$ , respectively, for ciNPT, and  $40.5 \pm 19.0$ ,  $42.1 \pm 25.3$ , and  $26.4 \pm 11.2$ , respectively, for control. Corresponding measures of oedema on Days 2, 6, and 9, quantified as percent increase in tissue thickness from baseline, were  $70\% \pm 0.33\%$ ,  $74\% \pm 0.37\%$ , and  $42\% \pm 0.36\%$ , respectively, for ciNPT, and  $82\% \pm 0.33\%$ ,  $87\% \pm 0.51\%$ , and  $49.4\% \pm 0.32\%$ , respectively, for control (Figure 6A,B). Further evidence of inflammation, as quantified by percent increase in lymph node volume from baseline on Days 2, 6, 9, were  $26\% \pm 0.38\%$ ,  $35\% \pm 0.55\%$ ,

and  $15\% \pm 0.53\%$ , respectively for ciNPT and  $50\% \pm 0.39\%$ ,  $51\% \pm 0.41\%$ , and  $40\% \pm 0.33\%$ , respectively for control.

### 3.3 | Lower Incidence/Severity of Seroma

Semi-quantitative histologic analysis showed similar levels of inflammation and tissue granulation at the incision site consistent with the surgical procedure and unrelated to either treatment. The most notable finding for the incision site was the presence of seroma/lymphocele formation in the deep aspect of the tissue. There was an increased incidence and intensity of deep seroma formation in the control versus ciNPT samples but differences in intensity scoring were not statistically significant ( $p=0.1675$ ). Deep seroma was observed in 7 of 8 control sites (mean score  $2.00 \pm 1.07$ ) versus 4 of 8 ciNPT sites (mean score  $1.13 \pm 1.25$ ) in the upper incision undermined area (Figure 7A) and 6 of 8 control ( $1.75 \pm 1.16$ ) versus 5 of 8 of ciNPT sites ( $1.25 \pm 1.28$ ) in the lower aspect of the incision near the suture line (Figure 7B). The seroma scores for both treatments were low in severity with the mean scores being mild (score of 2) to minimal (score of 1).

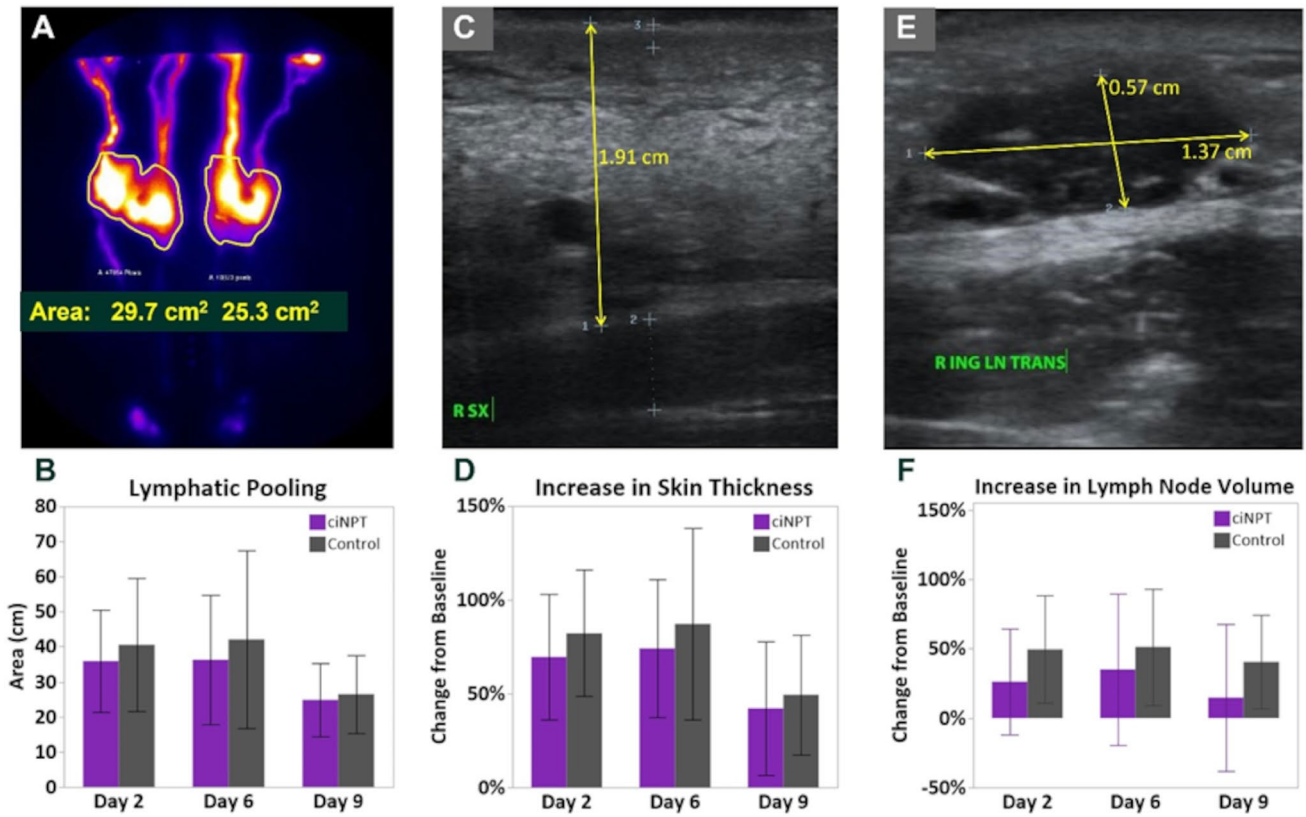


**FIGURE 6** | (A) Example image illustrating the quantification of the extent of lymphatic pooling (Fig 5, Day 2) and (B) plot illustrating the mean area over time. (C) Ultrasound image illustrating increase in oedema from baseline (measurement of tissue thickness from skin surface to muscle fascia) at the surgical site (Fig 3, Day 2) and (D) plot of the mean percent change of thickness by treatment over time. (E) Ultrasound image illustrating the measurement of the transverse height and width of the right inguinal lymph node (Fig 4, Day 6) and (F) plot of the mean percent change in lymph node volume from baseline. Error bars depict standard deviation.

### 3.4 | Increased Lymphatic Vessel Markers Closest to Draining Lymph Nodes

Similar levels of lymphatic vessel markers podoplanin and LYVE-1 were observed between treatments in the upstream and incision locations, and larger differences were seen in the downstream location but were not significant perhaps owing to the small sample size ( $n=8$ ). Downstream ciNPT podoplanin was  $488.4 \text{ ng/g} \pm 71.6$  versus  $363.8 \text{ ng/g} \pm 32.7$  for control;  $p=0.8805$ , and LYVE-1 was  $13.0 \pm 1.2 \mu\text{g/g}$  for ciNPT versus  $10.2 \pm 0.9 \mu\text{g/g}$  for control;  $p=0.0916$ . Further comparisons between locations showed higher levels of podoplanin and LYVE-1 for both ciNPT and control in the downstream location to be significantly higher than those found in upstream tissues. Steel-Dwass comparisons of location and treatment showed downstream ciNPT podoplanin levels were significantly higher ( $p < 0.05$ ) for both treatments compared with those upstream (Figure 8A). Downstream ciNPT podoplanin was 56% greater than the ciNPT upstream location ( $488.4 \text{ ng/g}$  total protein  $\pm 71.6$  and  $215.0 \pm 16.4$ , respectively;  $p=0.0448$ ) and 59% greater than control upstream ( $488.4 \text{ ng/g} \pm 71.6$  and  $201.6 \text{ ng/g}$ , respectively  $\pm 22.2$ ;  $p=0.0448$ ). Steel-Dwass comparisons of LYVE-1 showed downstream ciNPT to be significantly higher than both treatments at the upstream and incision locations ( $p < 0.03$ ). Downstream ciNPT (Figure 8B) was 53% higher than ciNPT upstream ( $12.9 \mu\text{g/g}$  total protein  $\pm 1.2$  and  $6.0 \pm 0.5$ , respectively;

$p=0.0171$ ) and 53% higher than control upstream ( $12.9 \mu\text{g/g} \pm 1.2$  and  $6.1 \pm 0.4$ , respectively;  $p=0.0121$ ) and 47% higher than ciNPT incision ( $12.9 \mu\text{g/g} \pm 1.2$  and  $6.8 \mu\text{g/g} \pm 0.7$ , respectively;  $p=0.0330$ ) and 49% higher than control incision ( $12.9 \mu\text{g/g} \pm 1.2$  and  $6.6 \mu\text{g/g} \pm 0.6$ , respectively;  $p=0.0239$ ).

## 4 | Discussion and Conclusion

Early adopters of negative pressure wound therapy believed that the mechanical removal of exudate from the wound was responsible for oedema reduction [30–32]. More recent observations of decreased incidence of seroma and oedema without a corresponding increase in fluid removal suggest that another intrinsic mechanism for decreased interstitial tissue fluid accumulation be responsible [9, 33]. In an earlier porcine study, Kilpadi and Cunningham noted that ciNPT reduced hematoma/seroma formation by 63% in treated sites as compared with control [34]. Isotope-labelled nanospheres were administered into undermined surgical sites. Following 4 days of therapy, 50% more isotope-labelled nanospheres were found to have migrated into the draining lymph nodes on the treated sides as compared with those on the control. The combination of reduced hematoma/seroma and increased number of nanospheres in lymph nodes draining from treated sites without concomitant fluid removal indicated that the lymphatic system played a key role [34].

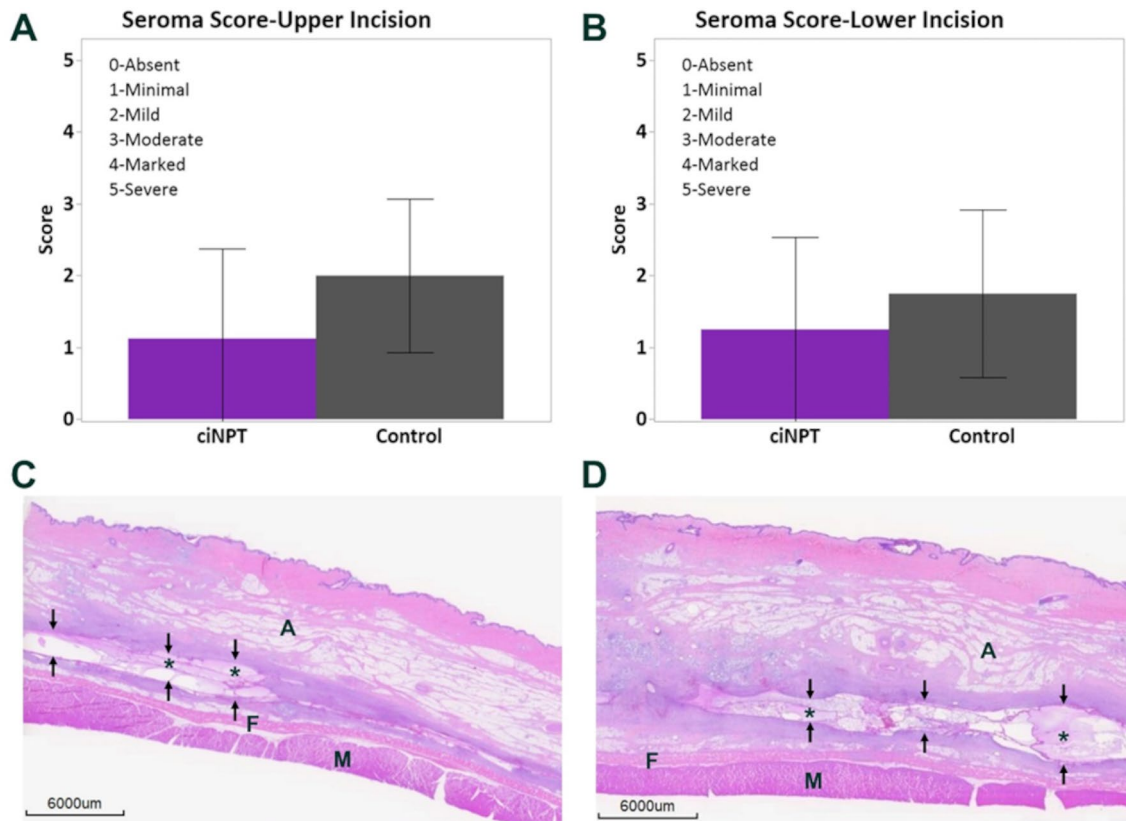


**FIGURE 7** | (A) Pathology scoring of deep seromas from upper aspect of incision site with undermining. (B) Pathology scoring of deep seromas from lower aspect of incision near suture line. Error bars depict standard deviation. Representative slides of (C) ciNPT site and (D) control site showing black arrows along the lining of deep seroma pocket with fluid filled serous/lymphatic fluid noted by asterisks. A = adipose tissue, F = deep fascial layer, M = deep muscle layer.

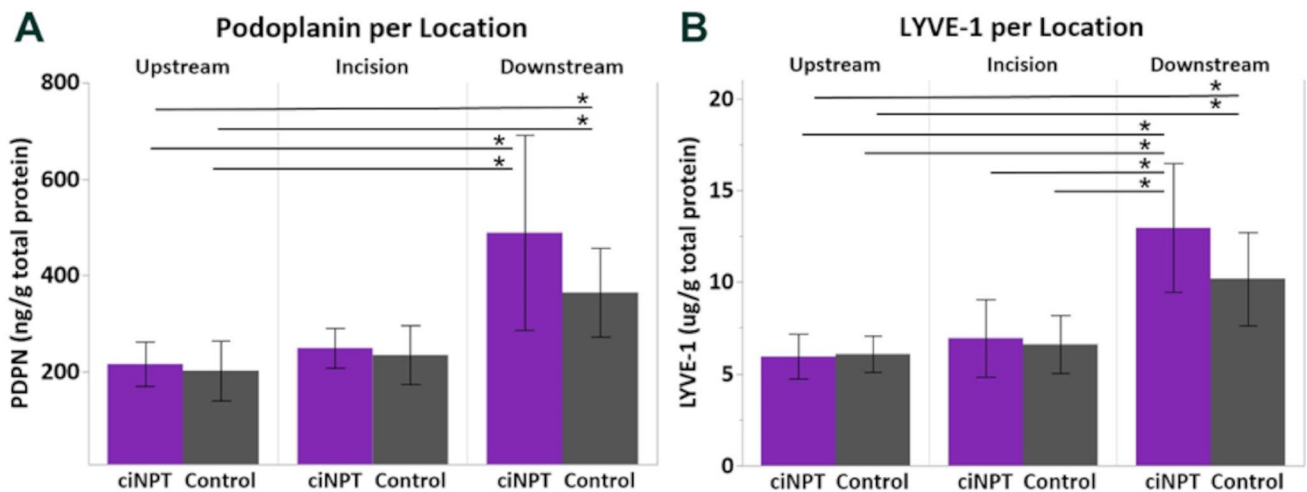


**FIGURE 8** | Lymphatic markers from biopsy samples taken upstream (cranial to incision), at the incision, and downstream (caudal to incision). (A) Podoplanin was significantly greater in both downstream treatments as compared with the upstream location, but not at the incision. (B) LYVE-1 was significantly higher in both downstream treatments as compared with the upstream location, and ciNPT downstream was also greater than both treatments at the incision. \* $p < 0.01$ .

The current report provides additional preclinical evidence of lymphatic involvement in reducing post-surgical oedema with the application of negative pressure over intact skin.

It was hypothesised that increased lymphatic activity induced by ciNPT could be directly observed and quantified using

NIRF-LI. A previous unpublished 2-animal pilot study showed faster rates of ICG-laden lymph pulses moving through ciNPT treated vessels compared with controls, but after careful examination, it was determined that variabilities existed in data collection which may have potentially affected the outcome. In some cases data was collected without dressings in place,

or with dressings from the previous visit in place, or after new dressings were placed. Since the pilot study did not evaluate differences with and without dressings, the significant increase in propulsion rates in both treated and control sites when negative pressure was in use was unexpected. Hence, the effect ciNPT versus a true untreated control could not be discerned in this study warranting investigation in a future study with separate control and treatment arms versus the bilateral/contralateral comparison presented in this work. We propose that, in addition to providing an effect immediately underneath the ciNPT dressing, ciNPT may have affected the contralateral control by mechanically stretching the skin from the control site towards the ciNPT site as the ciNPT dressing collapses under negative pressure thereby also opening dermal lymphatic capillaries on the control side to facilitate the passage of interstitial fluid into lymph vessels. Anchoring filaments connected to endothelial cells in lymphatic capillaries stretch due to increased interstitial fluid pressure or mechanical stimulation to allow for fluid transport through the lymphatic system [35–37]. Likewise, mechanical stretching of the skin under negative pressure may have allowed for fluid to pass readily into collecting vessels to promote slightly higher pumping rates on the control side. In addition, because lymphangiogenesis across the midline has been imaged in humans [38, 39] and in Fig 2 (Figure 2) of this study, regional ciNPT could influence watersheds outside of the treated area.

Despite the increased rate of control lymphatic activity as seen on Days 2, 6, and 9 compared with ciNPT, a corresponding decrease in oedema was not observed given greater lymphatic pooling at the surgical site, higher increase in tissue thickness, and greater incidence of seroma in controls. Lower levels of lymphatic pooling, decreased tissue thickness, and smaller lymph

node volumes in the ciNPT treatment may be attributed to more efficient clearance of post-surgical oedema.

While the determinants of pulsatile lymphatic activity are not yet fully understood, evidence suggests that they may be regulated in part by hydrostatic pressure [40]. Decreased lymphatic propulsion rate in ciNPT treated sites may be due to more efficient clearance of post-surgical oedema resulting in lower hydrostatic pressure. Reduced lymphatic pooling at ciNPT sites suggests less lymphatic congestion and supports this hypothesis.

In this work, use of NIRF-LI demonstrates that use of ciNPT significantly increases lymphatic pumping function and significantly increases lymphatic vessel density as indicated by LYVE-1 and PDPN in lymph draining tissues compared with other locations and suggests that ciNPT decreases interstitial fluid accumulation at incision sites. We hypothesise that ciNPT-induced forces on ECM enhance uptake within initial lymphatics by movement of the ECM-linked fibrils that open and close lymphatic endothelial cells. This action would allow passage of fluid, waste, and danger-associated molecular patterns (DAMPs) associated with cell death into the lymphatics that drain through the larger conducting and collecting lymphatic vessels into inguinal lymph nodes, illustrated in Figure 9. While the determinants of lymphatic pumping remain largely unknown, ciNPT mechanostimulation of lymphangions by virtue of enhanced fluid taken up by the lymphatics may be responsible for enhanced pumping, as also shown by NIRF-LI, to occur through conventional manual lymphatic drainage [26]. Whether activation of lymphatic smooth muscle cells occurs through increased lymphatic fluid load and/or mechanostimulation through sympathetic or autonomic mechanisms remains unknown. Nonetheless, our work clearly demonstrates ciNPT

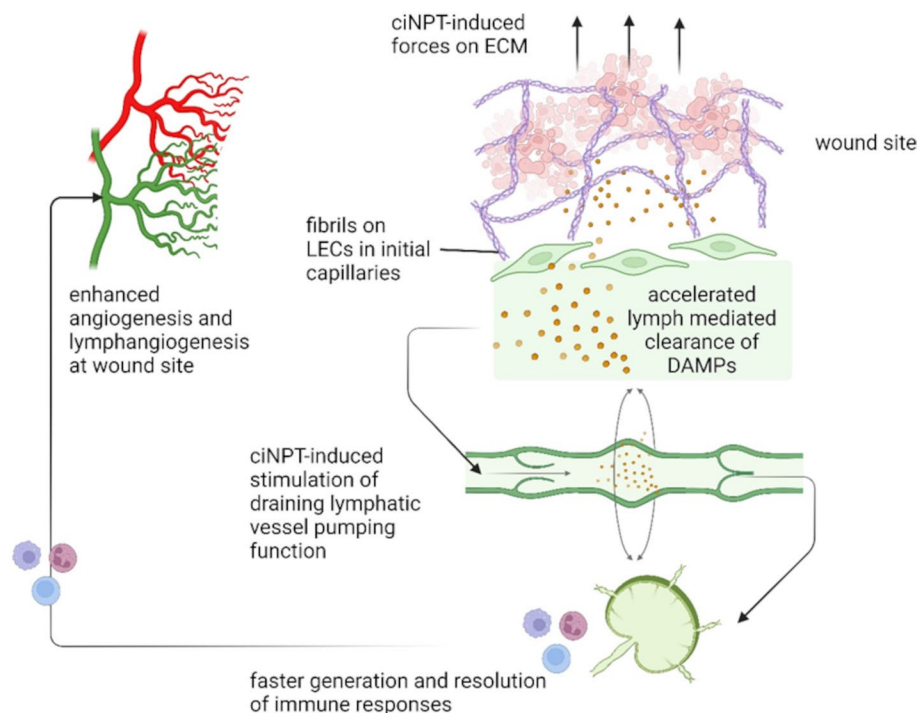


**FIGURE 9** | Illustration demonstrating how ciNPT acts on the ECM to stretch fibrils connected to lymphatic endothelial cells (LECs) (anchoring filaments) located in initial lymph capillaries opening gaps and facilitating passage of fluid, waste, and danger-associated molecular patterns (DAMPs) into the lymphatic vasculature and through the lymph nodes. Created in BioRender.

enhances lymphatic drainage. Because ciNPT action likely impacted the lymphatic watershed of the nearby, contralateral, untreated incision sites, our experimental design likely results in the relative attenuation of the impact of ciNPT. In addition, because clinical reports indicate improved systemic lymphatic function with regional manual lymphatic drainage [26], further testing of ciNPT treatment effects should have separate treated and untreated control cohorts. Despite the spill-over effects of ciNPT on the contralateral untreated sides, which may have prevented achieving statistical significance, our results suggest the treated side may have experienced greater lymphangiogenesis in draining tissues, reduced oedema at incision sites, and reduced lymph node volume after post-surgical initiation of ciNPT. Given that adaptive immune responses mounted within draining lymph nodes are essential to quell the initial innate responses to tissue injury and necessary for effective tissue regeneration, we expect that ciNPT-enhanced drainage to lymph nodes has the potential to accelerate tissue regenerative processes, as evidenced by reduced lymph node size 9–14 days after incision and ciNPT treatment.

### Acknowledgements

The authors would like to acknowledge Dr. Christopher Janssen, DVM for his efforts with the surgical animal model and ultrasound expertise as well as all laboratory animal staff at UT Health for the essential role they play as members of the research team. The authors would also like to acknowledge members of Solventum staff, Pedro Maldonado, Diwi Allen and Kathleen Derrick for their contributions to data quality control and Meredith Peratikos for her guidance with statistical analysis.

### Conflicts of Interest

Solventum employs some of the authors (M.S., S.M., and K.K.) and provided funding for the work. J.C.R., E.M.S., and the University of Texas Health Science Center at Houston have financial interests (patents) related to near-infrared fluorescence lymphatic imaging.

### Data Availability Statement

The data that support the findings of this study are available from the corresponding author upon reasonable request.

### References

1. P. D. McMaster and S. S. Hudack, "The Participation of Skin Lymphatics in Repair of the Lesions due to Incisions and Burns," *Journal of Experimental Medicine* 60, no. 4 (1934): 479–501, <https://doi.org/10.1084/jem.60.4.479>.
2. D. C. Fischer, A. Sckell, A. Garkisch, et al., "Treatment of Perioperative Swelling by Rest, Ice, Compression, and Elevation (RICE) Without and With Additional Application of Negative Pressure (RICE+) in Patients With a Unilateral Ankle Fracture: Study Protocol for a Monocentric, Evaluator-Blinded Randomized Controlled Pilot Trial," *Pilot and Feasibility Studies* 7, no. 1 (2021): 203, <https://doi.org/10.1186/s40814-021-00944-7>.
3. I. Klein, D. Tidhar, and L. Kalichman, "Lymphatic Treatments After Orthopedic Surgery or Injury: A Systematic Review," *Journal of Bodywork and Movement Therapies* 24, no. 4 (2020): 109–117, <https://doi.org/10.1016/j.jbmt.2020.06.034>.
4. D. Cagney, L. Simmons, D. P. O'Leary, et al., "The Efficacy of Prophylactic Negative Pressure Wound Therapy for Closed Incisions in Breast Surgery: A Systematic Review and Meta-Analysis," *World Journal of*

*Surgery* 44, no. 5 (2020): 1526–1537, <https://doi.org/10.1007/s00268-019-05335-x>.

5. J. Song, X. Liu, and T. Wu, "Effectiveness of Prophylactic Application of Negative Pressure Wound Therapy in Stopping Surgical Site Wound Problems for Closed Incisions in Breast Cancer Surgery: A Meta-Analysis," *International Wound Journal* 20, no. 2 (2023): 241–250, <https://doi.org/10.1111/iwj.13866>.

6. W. Xie, L. Dai, Y. Qi, and X. Jiang, "Negative Pressure Wound Therapy Compared With Conventional Wound Dressings for Closed Incisions in Orthopaedic Trauma Surgery: A Meta-Analysis," *International Wound Journal* 19, no. 6 (2021): 1319–1328, <https://doi.org/10.1111/iwj.13726>.

7. D. Zhang and L. He, "A Systemic Review and a Meta-Analysis on the Influences of Closed Incisions in Orthopaedic Trauma Surgery by Negative Pressure Wound Treatment Compared With Conventional Dressings," *International Wound Journal* 20, no. 1 (2023): 46–54, <https://doi.org/10.1111/iwj.13835>.

8. A. Lakhani, W. Jamel, G. E. Riddiough, C. S. Cabalag, S. Stevens, and D. S. Liu, "Prophylactic Negative Pressure Wound Dressings Reduces Wound Complications Following Emergency Laparotomies: A Systematic Review and Meta-Analysis," *Surgery* 172, no. 3 (2022): 949–954, <https://doi.org/10.1016/j.surg.2022.05.020>.

9. M. G. Jørgensen, N. M. Toyserkani, J. B. Thomsen, and J. A. Sørensen, "Prophylactic Incisional Negative Pressure Wound Therapy Shows Promising Results in Prevention of Wound Complications Following Inguinal Lymph Node Dissection for Melanoma: A Retrospective Case-Control Series," *Journal of Plastic, Reconstructive & Aesthetic Surgery: JPRAS* 72, no. 7 (2019): 1178–1183, <https://doi.org/10.1016/j.bjps.2019.02.013>.

10. J. P. Stannard, J. T. Robinson, E. R. Anderson, G. McGwin, D. A. Volgas, and J. E. Alonso, "Negative Pressure Wound Therapy to Treat Hematomas and Surgical Incisions Following High-Energy Trauma," *Journal of Trauma* 60, no. 6 (2006): 1301–1306, <https://doi.org/10.1097/01.ta.0000195996.73186.2e>.

11. K. C. Lin, Y. S. Li, and Y. W. Tarng, "Safety and Efficacy of Prophylactic Closed Incision Negative Pressure Therapy After Acute Fracture Surgery," *Injury* 51, no. 8 (2020): 1805–1811, <https://doi.org/10.1016/j.injury.2020.05.032>.

12. S. U. Eisenhardt, Y. Schmidt, J. R. Thiele, et al., "Negative Pressure Wound Therapy Reduces the Ischaemia/Reperfusion-Associated Inflammatory Response in Free Muscle Flaps," *Journal of Plastic, Reconstructive & Aesthetic Surgery: JPRAS* 65, no. 5 (2012): 640–649, <https://doi.org/10.1016/j.bjps.2011.11.037>.

13. M. S. Timmers, S. Le Cessie, P. Banwell, and G. N. Jukema, "The Effects of Varying Degrees of Pressure Delivered by Negative-Pressure Wound Therapy on Skin Perfusion," *Annals of Plastic Surgery* 55, no. 6 (2005): 665–671, <https://doi.org/10.1097/01.sap.0000187182.90907.3d>.

14. B. Z. Atkins, J. K. Tetterton, R. P. Petersen, K. Hurley, and W. G. Wolfe, "Laser Doppler Flowmetry Assessment of Peristernal Perfusion After Cardiac Surgery: Beneficial Effect of Negative Pressure Therapy," *International Wound Journal* 8, no. 1 (2011): 56–62, <https://doi.org/10.1111/j.1742-481X.2010.00743.x>.

15. C. Y. Xia, A. X. Yu, B. Qi, M. Zhou, Z. H. Li, and W. Y. Wang, "Analysis of Blood Flow and Local Expression of Angiogenesis-Associated Growth Factors in Infected Wounds Treated With Negative Pressure Wound Therapy," *Molecular Medicine Reports* 9, no. 5 (2014): 1749–1754, <https://doi.org/10.3892/mmr.2014.1997>.

16. N. Kairinos, A. M. Voogd, P. H. Botha, et al., "Negative-Pressure Wound Therapy II: Negative-Pressure Wound Therapy and Increased Perfusion. Just an Illusion?," *Plastic and Reconstructive Surgery* 123, no. 2 (2009): 601–612, <https://doi.org/10.1097/PRS.0b013e318196b97b>.

17. P. E. Banwell and L. Téot, "Topical Negative Pressure (TNP): The Evolution of a Novel Wound Therapy," *Journal of Wound Care* 12, no. 1 (2003): 22–28, <https://doi.org/10.12968/jowc.2003.12.1.26451>.

18. S. Kwon and E. M. Sevick-Muraca, "Mouse Phenotyping With Near-Infrared Fluorescence Lymphatic Imaging," *Biomedical Optics Express* 2, no. 6 (2011): 1403–1411, <https://doi.org/10.1364/BOE.2.001403>.
19. R. Sharma, W. Wang, J. C. Rasmussen, et al., "Quantitative Imaging of Lymph Function," *American Journal of Physiology. Heart and Circulatory Physiology* 292, no. 6 (2007): H3109–H3118, <https://doi.org/10.1152/ajpheart.01223.2006>.
20. R. Sharma, J. A. Wendt, J. C. Rasmussen, K. E. Adams, M. V. Marshall, and E. M. Sevick-Muraca, "New Horizons for Imaging Lymphatic Function," *Annals of the New York Academy of Sciences* 1131 (2008): 13–36, <https://doi.org/10.1196/annals.1413.002>.
21. J. C. Rasmussen, I. C. Tan, M. V. Marshall, C. E. Fife, and E. M. Sevick-Muraca, "Lymphatic Imaging in Humans With Near-Infrared Fluorescence," *Current Opinion in Biotechnology* 20, no. 1 (2009): 74–82, <https://doi.org/10.1016/j.copbio.2009.01.009>.
22. E. M. Sevick-Muraca, C. E. Fife, and J. C. Rasmussen, "Imaging Peripheral Lymphatic Dysfunction in Chronic Conditions," *Frontiers in Physiology* 14 (2023): 1132097, <https://doi.org/10.3389/fphys.2023.1132097>.
23. National Research Council, *Guide for the Care and Use of Laboratory Animals*, 8th ed. (Washington, DC: National Academies Press, 2011), 12910, <https://doi.org/10.17226/12910>.
24. R. Ito and H. Suami, "Lymphatic Territories (Lymphosomes) in Swine: An Animal Model for Future Lymphatic Research," *Plastic and Reconstructive Surgery* 136, no. 2 (2015): 297–304, <https://doi.org/10.1097/PRS.0000000000001460>.
25. T. Käser, "Swine as Biomedical Animal Model for T-Cell Research-Success and Potential for Transmittable and Non-Transmittable Human Diseases," *Molecular Immunology* 135 (2021): 95–115, <https://doi.org/10.1016/j.molimm.2021.04.004>.
26. I. C. Tan, E. A. Maus, J. C. Rasmussen, et al., "Assessment of Lymphatic Contractile Function After Manual Lymphatic Drainage Using Near-Infrared Fluorescence Imaging," *Archives of Physical Medicine and Rehabilitation* 92, no. 5 (2011): 756–764.e1.
27. Y. Ashitate, B. T. Lee, L. H. Ngo, et al., "Quantitative Assessment of Nipple Perfusion With Near-Infrared Fluorescence Imaging," *Annals of Plastic Surgery* 70, no. 2 (2013): 149–153, <https://doi.org/10.1097/SAP.0b013e31822f9af7>.
28. J. C. Rasmussen, S. Kwon, E. M. Sevick-Muraca, and J. N. Cormier, "The Role of Lymphatics in Cancer as Assessed by Near-Infrared Fluorescence Imaging," *Annals of Biomedical Engineering* 40, no. 2 (2012): 408–421, <https://doi.org/10.1007/s10439-011-0476-1>.
29. J. C. Rasmussen, I. C. Tan, M. V. Marshall, et al., "Human Lymphatic Architecture and Dynamic Transport Imaged Using Near-Infrared Fluorescence," *Translational Oncology* 3, no. 6 (2010): 362–372, <https://doi.org/10.1593/tlo.10190>.
30. L. P. Kamolz, H. Andel, W. Haslik, W. Winter, G. Meissl, and M. Frey, "Use of Subatmospheric Pressure Therapy to Prevent Burn Wound Progression in Human: First Experiences," *Burns: Journal of the International Society for Burn Injuries* 30, no. 3 (2004): 253–258, <https://doi.org/10.1016/j.burns.2003.12.003>.
31. L. X. Webb and H. C. Pape, "Current Thought Regarding the Mechanism of Action of Negative Pressure Wound Therapy With Reticulated Open Cell Foam," *Journal of Orthopaedic Trauma* 22, no. 10 Suppl (2008): S135–S137, <https://doi.org/10.1097/BOT.0b013e31818956ce>.
32. L. C. Argenta and M. J. Morykwas, "Vacuum-Assisted Closure: A New Method for Wound Control and Treatment: Clinical Experience," *Annals of Plastic Surgery* 38, no. 6 (1997): 563–576; discussion 577.
33. H. J. Cooper, G. C. Roc, M. A. Bas, et al., "Closed Incision Negative Pressure Therapy Decreases Complications After Periprosthetic Fracture Surgery Around the Hip and Knee," *Injury* 49, no. 2 (2018): 386–391, <https://doi.org/10.1016/j.injury.2017.11.010>.
34. D. V. Kilpadi and M. R. Cunningham, "Evaluation of Closed Incision Management With Negative Pressure Wound Therapy (CIM): Hematoma/Seroma and Involvement of the Lymphatic System," *Wound Repair and Regeneration* 19, no. 5 (2011): 588–596, <https://doi.org/10.1111/j.1524-475X.2011.00714.x>.
35. M. Skobe and M. Detmar, "Structure, Function, and Molecular Control of the Skin Lymphatic System," *Journal of Investigative Dermatology. Symposium Proceedings* 5, no. 1 (2000): 14–19, <https://doi.org/10.1046/j.1087-0024.2000.00001.x>.
36. L. V. Leak, "Studies on the Permeability of Lymphatic Capillaries," *Journal of Cell Biology* 50, no. 2 (1971): 300–323, <https://doi.org/10.1083/jcb.50.2.300>.
37. G. W. Schmid-Schönbein, "Mechanisms Causing Initial Lymphatics to Expand and Compress to Promote Lymph Flow," *Archives of Histology and Cytology* 53, no. Supplement (1990): 107–114, [https://doi.org/10.1679/aohc.53.Suppl\\_107](https://doi.org/10.1679/aohc.53.Suppl_107).
38. J. C. Rasmussen, I. C. Tan, S. Naqvi, et al., "Longitudinal Monitoring of the Head and Neck Lymphatics in Response to Surgery and Radiation," *Head & Neck* 39, no. 6 (2017): 1177–1188, <https://doi.org/10.1002/hed.24750>.
39. C. Gutierrez, R. J. Karni, S. Naqvi, et al., "Head and Neck Lymphedema: Treatment Response to Single and Multiple Sessions of Advanced Pneumatic Compression Therapy," *Otolaryngology-Head and Neck Surgery* 160, no. 4 (2019): 622–626, <https://doi.org/10.1177/0194599818823180>.
40. A. A. Gashev, M. J. Davis, M. D. Delp, and D. C. Zawieja, "Regional Variations of Contractile Activity in Isolated Rat Lymphatics," *Microcirculation* 11, no. 6 (2004): 477–492, <https://doi.org/10.1080/10739680490476033>.